

SEISMIC FRAGILITY DEVELOPMENT FOR BOTH ACCELERATION AND DRIFT SENSITIVE PIPING SYSTEMS

Ali BEITOLLAHI¹, Siavash SOROUSHIAN², Manos MARAGAKIS³

ABSTRACT

In recent earthquakes the failure of nonstructural elements including fire sprinkler piping systems has resulted in costly damages or, more importantly, has rendered buildings inoperable due to the flooding. Therefore, the need to understand how these systems perform during an earthquake is becoming increasingly important for the design of new buildings or retrofit of existing structures for higher performance objectives. However, few studies have been conducted on fire sprinkler piping systems to identify where they are vulnerable. Therefore, this study aims to fill in the gap in the current knowledge of the seismic response and fragilities of fire sprinkler piping systems by using previously developed and verified analytical methodology. To do so, ten different classes of piping systems (including variation in piping mechanisms, type of pipe joints, bracing systems) are analytically developed based on an actual piping layout with more than 900 pipe joints and 400 supporting elements. Fully nonlinear behavior of pipe joints, supporting hangers and braces are incorporated in this study using OpenSees simulation platform. Fragility curves for riser pipes which are known to be the drift sensitive elements are obtained from the rotational capacity of their joints. Component and system level fragility curves are then developed for acceleration sensitive piping systems under 192 synthetically developed three dimensional floor motions. It was found that drift sensitive components constructed from threaded joints are more vulnerable, while acceleration sensitive components built from grooved fitting joints are more fragile compared to the other piping systems.

Keywords: Nonstructural Systems; Fire sprinkler piping system; Seismic fragility analysis; Analytical simulation

1. INTRODUCTION

The seismic performance of critical facilities such as power plants, hospitals, and industrial units depends not only on the performance of the structural systems, but also on the functionality of their nonstructural systems, specifically fire sprinkler piping systems. Taghavi and Miranada (2013) showed that damages resulting from the malfunction of nonstructural systems or their direct failure, were much greater than those related to the structural damages. Past earthquakes have shown pervasive damage to fire sprinkler piping systems as well as other nonstructural components.

Various failure modes were identified in fire sprinkler systems such as failure of fasteners and anchorages, breakage of sprinkler heads and leakage of pipe joints. Nearly all of these failure types have been observed in past earthquakes including the 1964 Alaska Earthquake, the 1971 San Fernando Earthquake, the 1989 Loma Prieta Earthquake, 1994 Northridge earthquake (Soroushian et al. 2011), 2010 Chile earthquake (Miranda et al. 2012), 2011 Tohoku Pacific Earthquake (Mizutani et al. 2012). However, the complex behavior of these interacting piping systems were greatly remained unknown due to the insufficient historical observations.

¹Head of Engineering and Seismology and Risk Department, Road, Housing, and Urban Development Research Center, Tehran, Iran, beitollahi@bhrc.ac.ir

²Assistant Professor, Faculty of Civil Engineering, K.N. Toosi University of Technology, Tehran, Iran, ssoroushian@kntu.ac.ir

³Dean of Engineering, Department of Civil and Environmental Engineering, University of Nevada, Reno, USA, maragaki@unr.edu

Over the last 20 years, several component and system level experiments (Antaki and Guzy 1998; Zaghi et al. 2012; Tian et al. 2014; Soroushian et al. 2012; Tian 2012; Jenkins et al. 2017) were performed on piping systems to provide more quantitative and qualitative data in addition to the historical data. As a result of these experiments, several experimentally-validated analytical models (Martinez and Hodgson 2007, Soroushian et al. 2011, Ju and Gupta 2012, Zaghi et al. 2012, Soroushian et al. 2015a, Soroushian et al. 2015b) were developed and used for generating fragility curves of sprinkler piping systems. However, as most of these analytical fragility studies were limited to their experimental setup or very few variations, a generic piping model with several design and functionality details scenarios were used in this study to overcome this limitation.

In this study, a brief description of previously tested sprinkler piping components along with their numerical models is presented. Afterwards, capacity values of different piping components are provided followed by the fragility methodology used here. Fragility parameter of riser pipes, which are known to be the drift sensitive components of a piping system, are then proposed for both threaded and grooved fitted piping joints. The numerical model of an adopted piping layout is discussed and ten different design scenarios are presented in detail. Fragility curves for acceleration sensitive systems are then developed under to 96 artificial triaxial floor acceleration histories. The effect of each design variations is then highlighted through these system level fragility curves.

2. COMPONENTS OF A FIRE SPRINKLER PIPING SYSTEM

A typical fire sprinkler piping system is composed of a water pressure tank, pipe runs, sprinkler heads, hangers, braces, and restrainers. Pressure tanks provide enough pressure behind the water in a system. Sprinkler heads spray the pressurized water onto an area in case of fire or smoke. Pipe runs are composed of: 1) risers: vertical supply pipes; 2) main runs: pipes that supply branch line water; 3) branch lines: provide drop pipe water; and drops: armover or straight drops that supply sprinkler head water. Hangers carry the dead weight of a piping system. Braces resist the seismic load of a piping system. Braces can be solid or tension-only (cable) braces. Wire restrainers limit the displacement movement of branch lines. A summary of different fire sprinkler piping components is presented in Figure 1.



Figure 1. Different components of a typical fire sprinkler piping system

3. METHODOLOGY OF SEISMIC FRAGILITY ANALYSIS

The seismic fragility is a probabilistic representation of engineering demand parameters (*EDPs*) exceeding specified capacities or limit states, given intensity measures (*IMs*). In this study, the relationship between several *EDPs* including pipe joint rotations and component forces, and peak floor

acceleration or drift as the IM are approximately represented with the log-normal cumulative distribution function shown in Equation 1 (Nielson and DesRoches 2007):

$$P(EDP \geq C|IM) = \Phi \left(\frac{\ln(S_d/S_c)}{\sqrt{\beta_{EDP|IM}^2 + \beta_C^2}} \right) \quad (1)$$

where S_d = median of the demand as a function of IM ; S_c = median estimated capacity; $\beta_{d|IM}$ = logarithmic standard deviation of the demand with respect to the IM ; β_c = logarithmic standard deviation of component capacities; and $\Phi[\cdot]$ = standard normal cumulative distribution function.

The seismic vulnerability of an acceleration sensitive piping system is assessed by combining the effects of the various piping components using a joint probabilistic seismic demand model (JPSDM) (Nielson and DesRoches 2007). A JPSDM is developed by assessing the demands placed on individual components (marginal distribution) through regression analysis. A covariance matrix is calculated by estimating the correlation coefficients between the demands placed on the various components. Using the capacity parameters and the JPSDM, Equation 2 can be evaluated using a Monte Carlo simulation

$$P[Fail_{system}] = \cup_{i=1}^n P[Fail_{Component-i}] \quad (2)$$

where the probability that the piping system will exceed a particular damage state, $P[Fail_{system}]$, is the union of the probabilities that each of the components will exceed that same damage state, $P[Fail_{Component-i}]$ (Nielson and DesRoches 2007). Three system damage states, Slight, Moderate, and Extensive, were defined by combining the previously defined component damage states.

4. FRAGILITY CURVES FOR DRIFT SENSITIVE PIPE RUNS

Riser pipes are recognized as the most important and common type of vertical pipe runs in fire sprinkler piping systems. However, other types of vertical pipe run such as wall mounted pipes can be used in a piping system. As mentioned before, vertical pipes are mostly drift sensitive part of a fire sprinkler piping system. Consequently, the assessment of seismic vulnerability of riser pipes is a crucial step for overall performance of piping systems. The steps that were implemented in this study to generate vertical pipes fragility curves are: 1) determine the pipe joint damage states, 2) relate the pipe joint rotational damage states to story drift ratio damage states, and 3) calculate the fragility parameters based on median and logarithmic standard deviation of damage states.

According to the work done by Tian et al. (2014), the proposed fragility curves are based on pipe joint rotation as IM . However, an appropriate transition from rotational capacities to story drift ratio as an intensity measure can convert these plots to be more applicable with respect to levels of structural deformation. Assuming that the rotation on vertical pipes imposed by building deformation (drift) is only concentrated at end joint rotations, simply, the joint rotation can be related to story drift ratio. The following assumptions have been made: 1) flexural and shear deformation of pipe segments is negligible; and 2) the top and bottom of risers at each floor is fixed by solid sway braces. Therefore, as shown in Figure 2, the vertical joint rotation can be converted to story drift ratio as:

$$\theta_{RJ} \times 100 \cong \frac{\Delta}{H} (\%) \quad (3)$$

where θ_{RJ} , Δ , and H are riser joint rotation, building deformation, and story height, respectively. Using the mentioned relation and assumptions, pipe joint damage states based on rotation can be converted to damage states presented in Table 1 based on inter-story drift ratio.

By using Equation 1, assuming the uniform distribution of IM (0 to 4% drift) and assuming $\beta_{D|IM} = 0$ (other values can be used), values presented in Table 1 can be used as median and dispersion values for the seismic fragility curves of the piping components under structural inter-story drift ratios. It should be mentioned that since pipe diameters larger than 2 inches are more common to use as riser pipes, fragility curves for drift sensitive components are developed for pipe diameters larger than 2 inches.

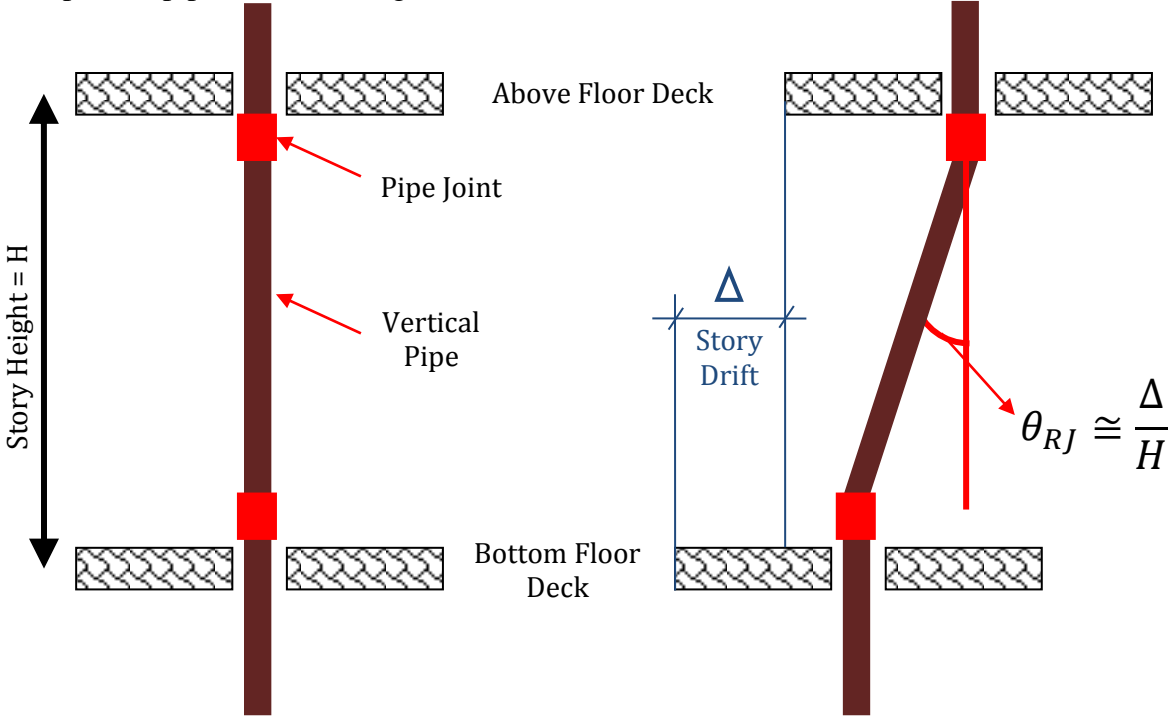


Figure 2. Schematic relation of riser joint rotation and inter-story drift

Table 1. Damage states of pipe joints rotation.

Pipe Diameter	Slight	Moderate	Extensive	Dispersion	Slight	Moderate	Extensive	Dispersion
	Median (rad.)				β _c			
					Median (Drift (%))			
THREADED								
3/4" Pipe	0.005	0.023	0.04	0.206	0.5	2.3	4	0.206
1" Pipe	0.005	0.018	0.031	0.146	0.5	1.8	3.1	0.146
1.25" Pipe	0.005	0.014	0.023	0.133	0.5	1.4	2.3	0.133
1.5" Pipe	0.005	0.013	0.02	0.12	0.5	1.3	2	0.12
2" Pipe	0.005	0.0094	0.014	0.094	0.5	0.94	1.4	0.094
2.5" Pipe	0.005	0.009	0.013	0.125	0.5	0.9	1.3	0.125
3" Pipe	0.005	0.008	0.011	0.155	0.5	0.8	1.1	0.155
3.5" Pipe	0.005	0.008	0.01	0.186	0.5	0.8	1	0.186
4" Pipe	0.005	0.01	0.01	0.216	0.5	1	1	0.216
5" Pipe	0.005	0.006	0.007	0.21	0.5	0.6	0.7	0.21
6" Pipe	0.005	0.006	0.006	0.204	0.5	0.6	0.6	0.204
GROOVED								
2" Pipe	0.015	0.05	0.077	0.17	1.5	5	7.7	0.17
2.5" Pipe	0.013	0.026	0.038	0.14	1.3	2.6	3.8	0.14
3" Pipe	0.01	0.019	0.029	0.11	1	1.9	2.9	0.11
3.5" Pipe	0.008	0.016	0.024	0.079	0.8	1.6	2.4	0.079
4" Pipe	0.005	0.01	0.021	0.049	0.5	1	2.1	0.049
5" Pipe	0.006	0.011	0.017	0.049	0.6	1.1	1.7	0.049
6" Pipe	0.005	0.01	0.014	0.049	0.5	1	1.4	0.049

As shown in Figure 3, in all pipe diameters, these curves indicate that threaded joints are more vulnerable compared to grooved joints. The curve differences are reduced when the pipe diameters are increased. Also these curves reveal that the overall probability of dripping (moderate damage state) in threaded joints are occurred in drift ratios less than 1%. Also

Figure 3 demonstrates that the overall probability of leakage (extensive damage state) in threaded joints was observed in drift ratios less than 1%. The probability of leakage in grooved connections for small pipe diameters (less than 3 inches) is very low. However, in larger pipe diameters, the probability of leakage in grooved joints was high in drift ratios around 1.5 %. Therefore, using flexible coupling can improve the riser pipes either with grooved or threaded joints

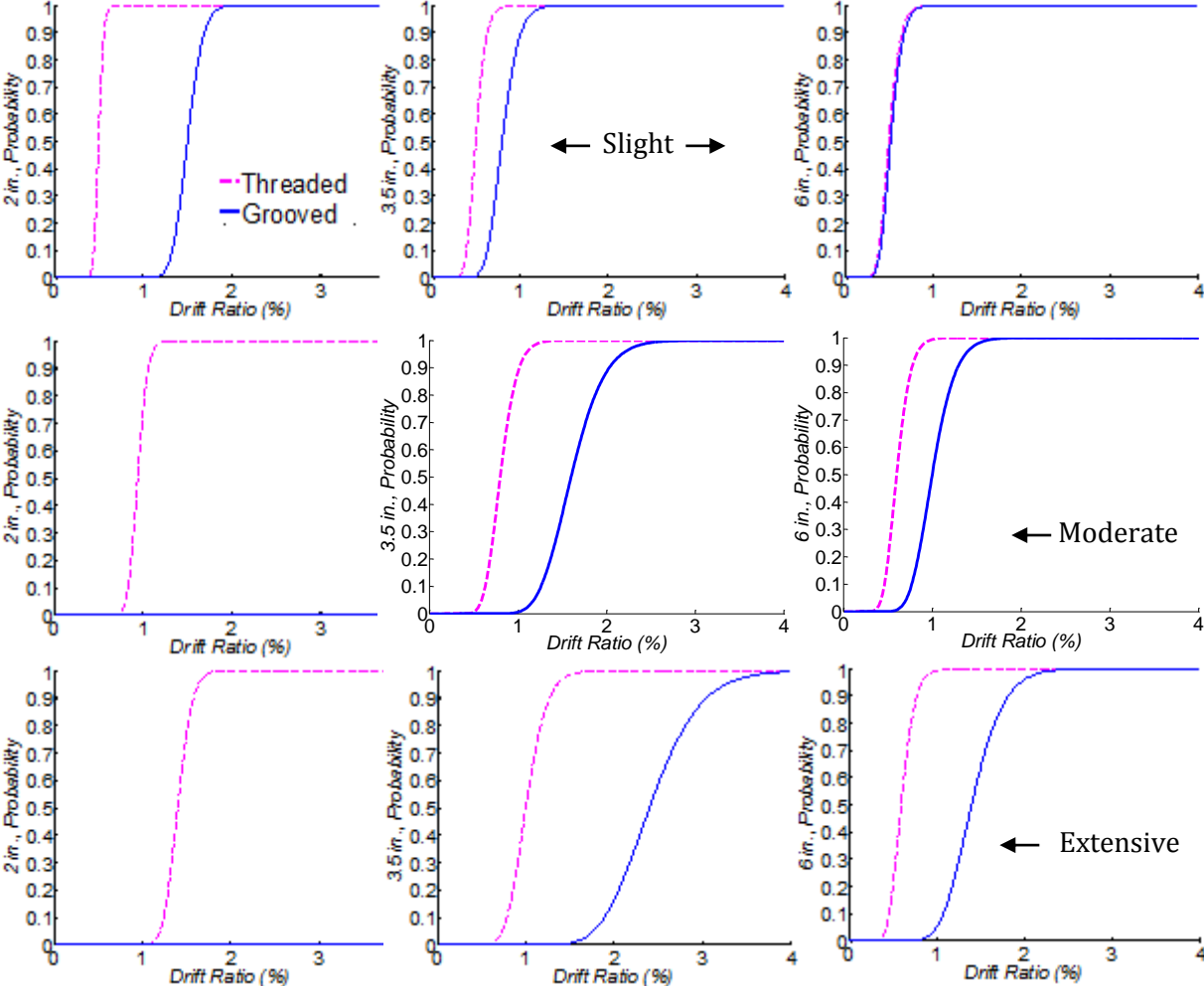


Figure 3. Fragility curved for different riser pipe diameters

5. FRAGILITY CURVES FOR ACCELERATION SENSITIVE PIPING SYSTEMS

The steps taken for generating the seismic fragility parameters of acceleration sensitive piping systems are presented in the following contents. In summary, the modeling methodology and the generation of piping demands for a piping layout borrowed from the UCSF hospital building will be presented. Then the seismic fragility curves for ten different piping systems will be presented. Finally, a discussion will be given on the performance of these piping systems.

5.1 Analytical Model of a Fire Sprinkler Piping System

The piping system shown in Figure 4 covers an area of approximately 17000 sf. It is 250 ft. long and 176 ft. wide and has more than 900 threaded joints (649 1-in., 185 1.25-in., 28 1.5-in., 7 2-in., 41 2.5-in., 34 3-in., and 29 4-in. diameter joints). A plenum height (the distance between the supporting structural floor and the ceiling system) of 4 ft. is used. The piping

system is suspended 2.5 ft below the supporting floor, thus the sprinkler drops are 1.5 ft. long. The sprinkler piping system is connected and braced to the supporting floor with 1-in. diameter longitudinal and lateral pipe sway braces, 3/8-in. all-threaded hangers, and 12-gauge wire restraints. The sway braces and wire restraints are oriented at 45-degree angles with respect to the plane of the supporting floor.

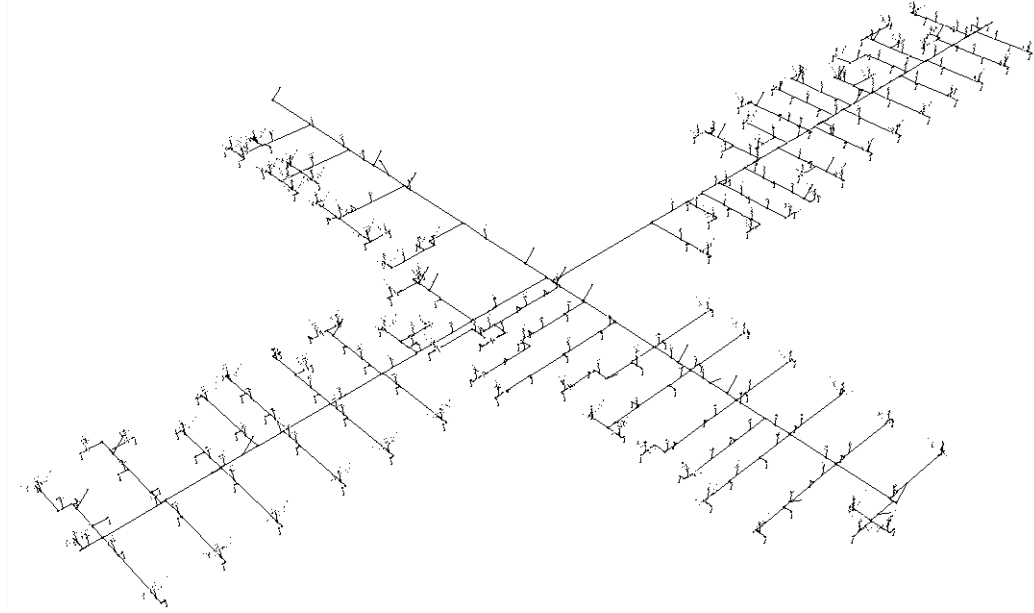


Figure 4. 3-D view of UCSF medical center sprinkler piping system

In this study, several typical design variables in addition to two types of generated floor motions were considered to produce 10 different piping scenarios (cases). The considered design variables in piping systems are: 1- Threaded versus grooved main run connections; 2- Solid versus cable bracing; 3- Wet versus dry piping system; 4- With and without restrainers for armover pipes; 4- Uniform versus log-normally generated floor motions. Table 2 presents different piping cases and their associated variables.

Table 2. Considered Parameters in Piping System Cases.

Case #	Main Run		S_{DS} Distribution		Piping System		Restrainer on Armovers		Bracing	
	Threaded	Grooved	Uniform	Lognormal	Wet	Dry	Yes	No	Solid	Cable
1	✓	✗	✓	✗	✓	✗	✓	✗	✓	✗
2	✓	✗	✗	✓	✓	✗	✓	✗	✓	✗
3	✓	✗	✓	✗	✗	✓	✓	✗	✓	✗
4	✓	✗	✓	✗	✓	✗	✗	✓	✓	✗
5	✓	✗	✓	✗	✓	✗	✓	✗	✗	✓
6	✗	✓	✓	✗	✓	✗	✓	✗	✓	✗
7	✗	✓	✗	✓	✓	✗	✓	✗	✓	✗
8	✗	✓	✓	✗	✗	✓	✓	✗	✓	✗
9	✗	✓	✓	✗	✓	✗	✗	✓	✓	✗
10	✗	✓	✓	✗	✓	✗	✓	✗	✗	✓

The analytical model of the piping subsystem was developed in OpenSees (2017). The pipes, including the main runs, branch lines, and sprinkler drops were modeled with Force-Based Beam-Column (OpenSees 2017) elements using the elastic gross section properties of the pipes and an elastic material with steel material properties. Grooved and threaded hinges were

modeled using the parameters developed and can be found in Soroushian (2015a, 2015b). To accommodate flexural yielding of the hanger bars, they were modeled using Force-Based Beam-Column elements with a nonlinear fiber-section consisting of the Giuffre-Menegotto-Pinto steel material (CEB 1996). This material is implemented in OpenSees as Steel02 material model. A modulus of elasticity of 29,000 ksi, yield strength of 85 ksi (Goodwin et al. 2005), and a hardening ratio of 1% were assigned to the hanger material. These hangers are pinned to the pipes and are fixed at their far ends. The wire restrainers modeled using truss elements, coupled with a tension only elastic-perfectly plastic (EPP) gap material with the modulus of elasticity of 29,000 ksi and tensile yield strength of 80 ksi (USG 2006). The rigid seismic braces were modeled with force-based beam-column elements using the elastic section properties of the 1-in. pipe. The connection of the solid braces was assumed to be rigid at both ends. The mass of the piping system was determined using the wet or dry weight of the pipes with an additional mass of 0.5 lb for each sprinkler head. The mass and weight of the system were concentrated at the nodal points.

A real-time element removal algorithm was incorporated in the analyses to capture the progression of damage to the piping system during seismic excitations. The element removal algorithm enables the model to redistribute the forces after failure occurs in an element using the remove element command in OpenSees (2017). This algorithm was set to remove the wire restrainers after reaching their rupture capacity, 0.4 kips from USG (2006). The failure algorithm for pipe hangers was set based on the minimum requirement by NFPA13 (2011), which is five times the weight of the water-filled pipes, plus 250 lb. A Rayleigh damping was used in the piping model and 3% damping was assigned to the first and third modes of vibration.

5.2 Generation of Floor Motions

The seismic response of the piping system was evaluated using two suites of 96 synthetic triaxial floor acceleration histories. The input motions were developed by Soroushian (2013) using the spectrum matching procedure. Acceleration spectra were produced following ICC-AC156 (ICC 2010) and ASCE/SEI 7-16 (ASCE 2016) for the horizontal and vertical acceleration parameters, respectively. The suites of motions were generated for uniform and log-normal distribution of design earthquake spectral response acceleration at short period (S_{DS}) values varying from 0.1 to 3 g and five different floor elevation ratios of 0, 0.25, 0.5, 0.75, and 1.0, considering site classes D, E, and F. The peak floor accelerations and the median 16th, 84th, and 97th percentile of the 5% damped elastic spectrum of uniform and log-normally distributed motions for the horizontal components are presented in Figure 5.

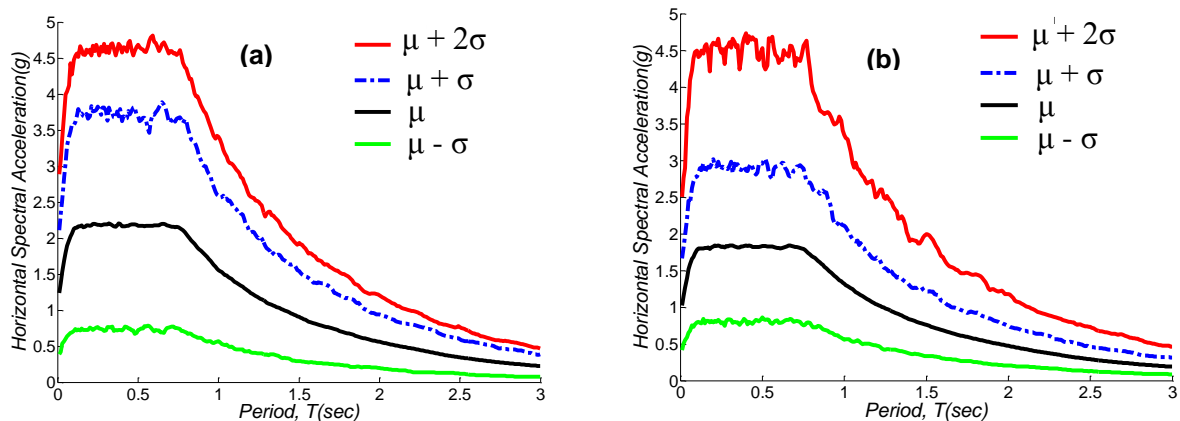


Figure 5. Horizontal spectral floor acceleration with (a) uniform S_{DS} distribution; (c) log-normal S_{DS} distribution

5.3 Development of Fragility Curves

Same as before, three damage states named Slight, Moderate, and Extensive were defined for the pipe components, which their associated values were presented in Table 1. The damage states of the pipe hangers and wire restrainers were determined by the median percentage of failed hangers or wire restrainers. Three damage states were defined for the percentage of failed hangers and wire restrainers. DS1 represents a 5% loss of hangers and a 10% loss of restrainers, DS2 represents a 10% loss hangers and a 20% loss of restrainers, and DS3 represents a 15% loss of hangers and a 30% loss of restrainers. A constant value of 0.4 was assigned to logarithmic standard deviation for pipe hangers and wire restrainers (Soroushian 2013).

Power-law regression and a single value for dispersion was used to characterize demand parameters in the fragility analysis of nonstructural components (Ramanathan 2012). Regression analyses were performed on following response data: (1) wire restrainer forces, (2) hanger forces, (3) rotation at armovers (horizontal pipes that supply water for only one sprinkler head), (4) the maximum rotations at the joints of a branch line, and (5) rotation of fittings on the main runs. The regression results were used to estimate the median demand, S_d , and the logarithmic standard deviation of the demand for each component, $\beta_{d|IM}$, using Equations 3 and 4 (Cornell et al. 2002):

$$S_d = aIM^b \quad (3)$$

$$\beta_{d|IM} \cong \sqrt{\frac{\sum_{i=1}^N [\ln(d_i) - \ln(aIM^b)]^2}{N-2}} \quad (4)$$

where d_i = peak demand, corresponding to the i^{th} floor motion out of the total N motions. Figure 6 shows a sample ratio of failed wire restrainers and the rotational demand of 2.5-in. pipe joints with respect to peak floor acceleration (PFA) for case 4 piping system.

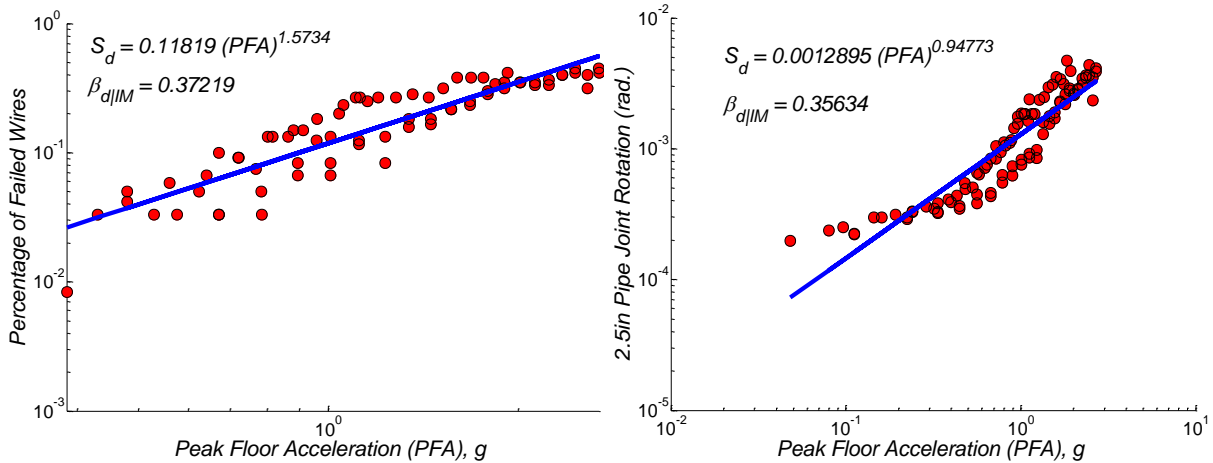


Figure 6. Sample probabilistic seismic demand: (a) percentage of failed wires, (b) 2.5 in. pipe joint rotation (rad.), Case 4

After calculating the demand and capacity parameters of the piping components, fragility curves for components and systems can be generated by utilizing Equations 1 and 2. It should be noted that System level fragility curves were developed for four different configurations: (1) All, considering all the components of the piping system, (2) w/o Armovers, removing armover demands from joint probabilistic seismic demand model (JPSDMs), (3) w/o Main Runs, removing main run demands from JPSDMs, and (4) w/o Main Runs & Armovers,

removing both main run and armover demands from JPSDMs. Sample component fragility curves for case 7 and system fragility curves for case 9 are presented in Figures 7 and 8, respectively.

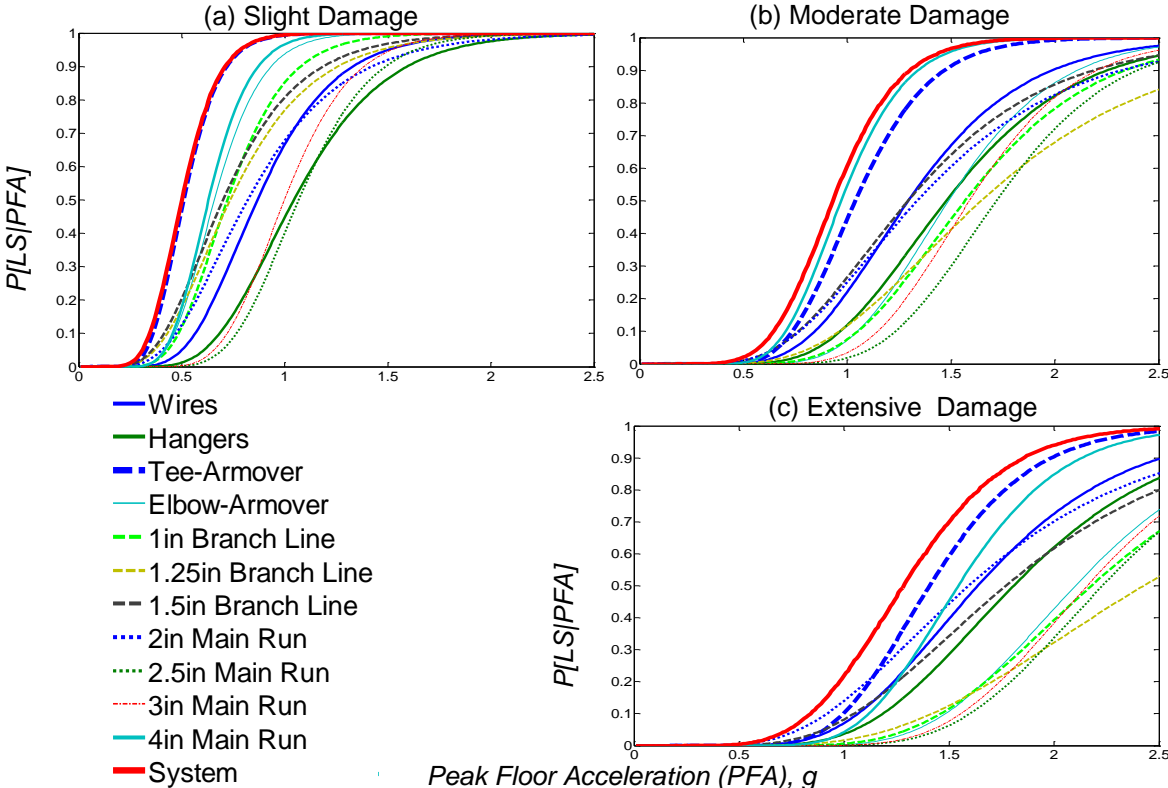


Figure 7. Component fragility curves for piping system of case 7

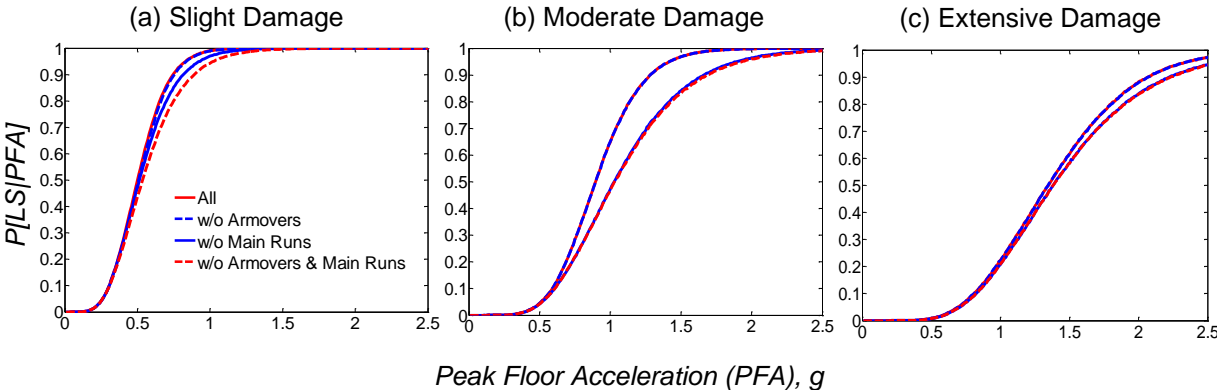


Figure 8. system fragility curves for different piping system condition of case 9

A simple comparison was made between the median PFA of all the piping cases considering all components, which is shown in Figure 9. This figure shows that, in all damage states, dry piping systems are the least vulnerable piping systems, which is due to elimination of mass of water from the piping system (green colored bars). The piping systems with cable braces were found to be the most vulnerable piping systems (red colored bars). The failure of cable braces was always found to be the dominant damage in system level fragilities. However, the results of this may be considered subjective, as the cable braces were never removed during response history analysis. Moreover, the damage states of cable braces can be changed based on

accurate cost and repair time estimation of cable braces.

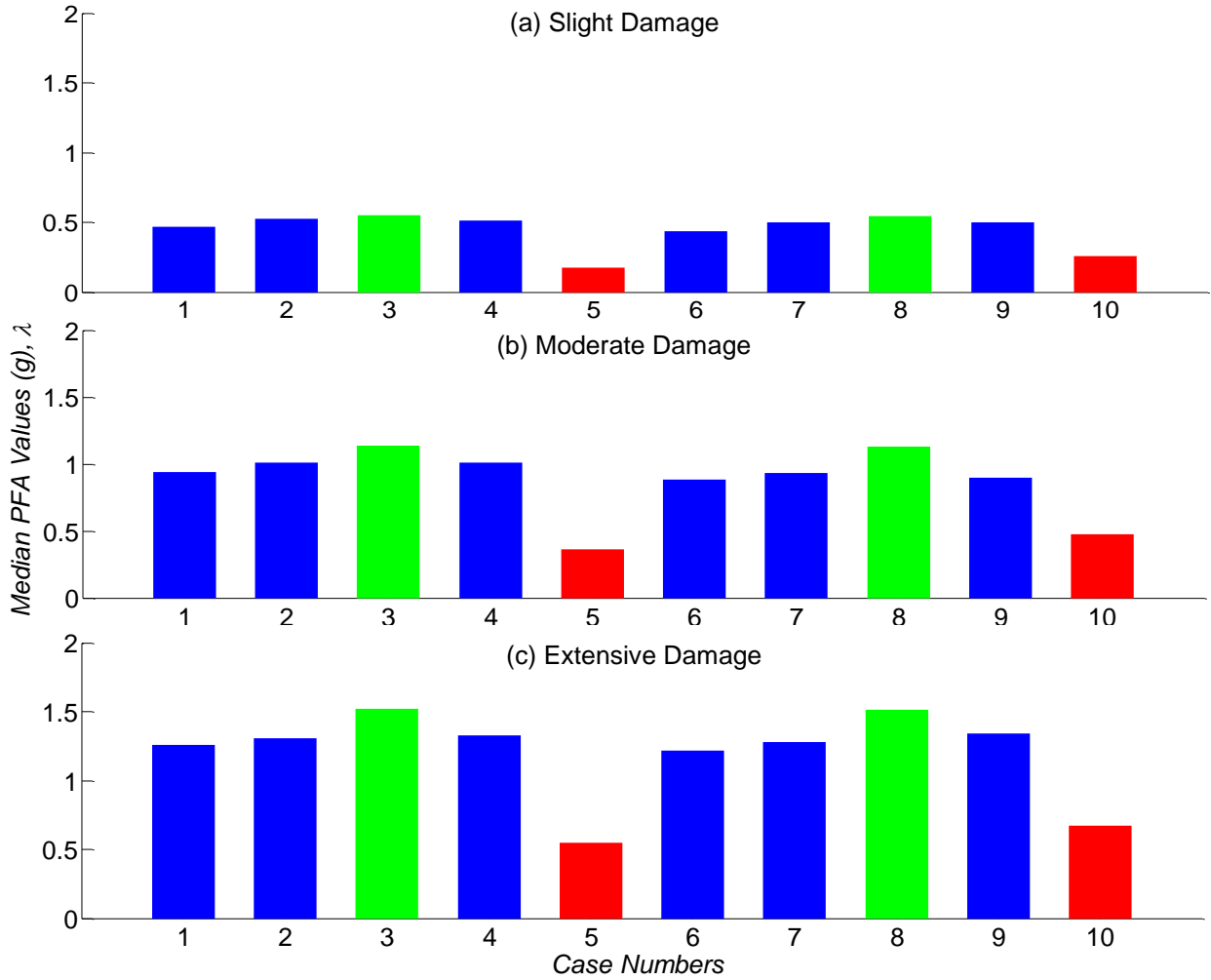


Figure 9. Comparison of median PFA values for all piping cases considering all components

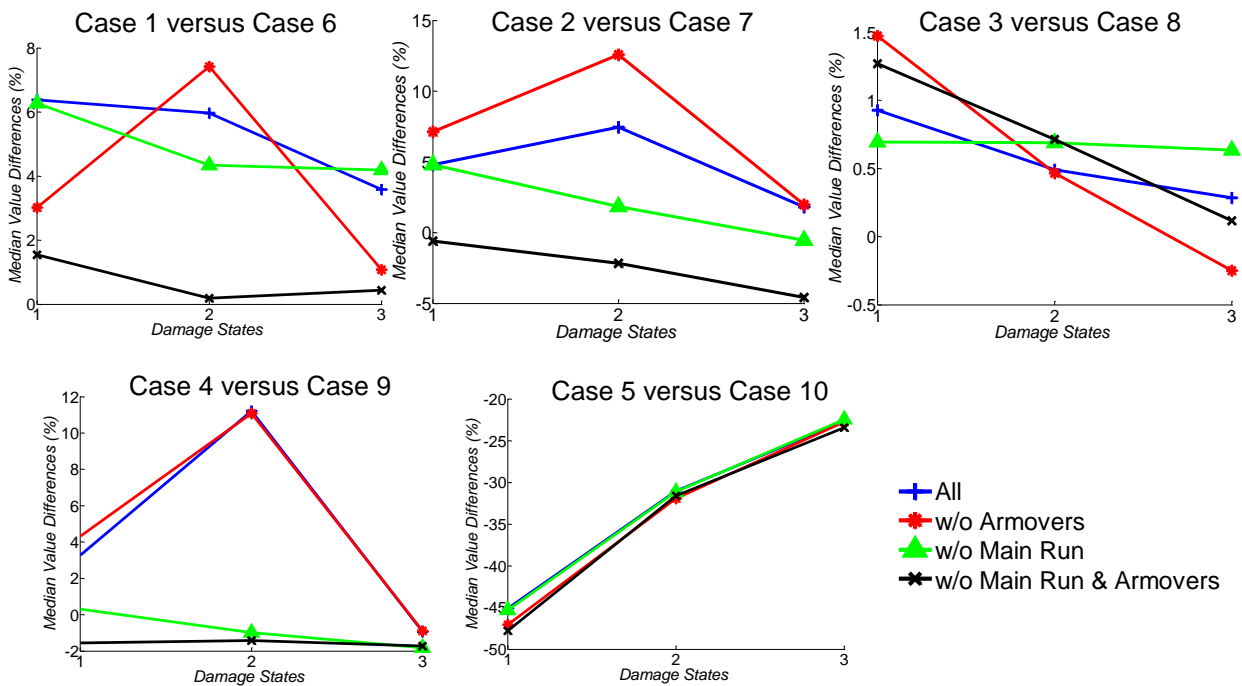


Figure 10. System median value differences considering main run joint variation

Similar approach was used to study the effect pipe joint types on the overall performance of fire sprinkler piping systems by using median fragility values. Figure 10 shows that in all piping systems and all cases (except with cable bracing), piping systems with grooved main run connections were slightly more fragile. Figure 10 shows that the differences in piping systems without main run consideration were the smallest. In the piping system with cable bracing, the piping system with threaded joints was found to be more fragile, which is not governed by joint rotation and only follows the percentage of bracing failure.

6. CONCLUSIONS

A fire sprinkler system layout incorporating a variety of common sprinkler piping components was adopted and modeled in OpenSees simulation platform. The modelling technique used in this study was based on previously developed and validated component and subsystem level models. Seismic fragility curves were generated by subjecting ten different design cases of this comprehensive three-dimensional model to two suites of artificial triaxial floor motions. The highlighted findings from this study was: 1) drift sensitive pipe runs with threaded joints are the most vulnerable components, 2) piping systems with grooved joints are the most fragile systems compared to the others, 3) in all damage states, dry piping systems are the least vulnerable piping systems and 4) piping systems with cable braces were found to be the most vulnerable piping systems.

7. ACKNOWLEDGMENTS

This material is based upon work partially supported by the National Science Foundation and Iranian Road, Housing, and Urban Development Research Center. Any opinions, findings, conclusions, or recommendations expressed in this document are those of the investigators and do not necessarily reflect the views of the sponsors. The authors are especially grateful to A. Gupta for providing the piping plan.

8. REFERENCES

- American Society of Civil Engineers (ASCE). (2016). Minimum design loads for buildings and other structures. *ASCE/SEI 7-16*, Reston, VA.
- Antaki, G., and Guzy, D. (1998). Seismic testing of grooved and threaded fire protection joints and correlation with NFPA seismic design provisions. *ASME, PVP-Vol. 364*, 624.
- Comite Euro-International du Beton (CEB). (1996). RC elements under cyclic loading, *state of the art report*, Thomas Telford, London.
- Cornell, A. C., Jalayer, F., Hamburger, R. O., and Foutch, D. A. (2002). Probabilistic basis for 2000 SAC federal emergency management agency steel moment frame guidelines. *J. Struct. Eng.*, 10.1061/(ASCE)0733-9445(2002)128:4(526), 526–533.
- Goodwin, E., Maragakis, M., Itani, A., and Luo, S. (2005). Experimental evaluation of the seismic performance of hospital piping subassemblies. *Rep. No. CCEER-05-5, Center for Civil Engineering Earthquake Research*, Dept. of Civil Engineering, Univ. of Nevada, Reno, NV.
- Jenkins, C., Soroushian, S., Rahmanishamsi, E., Maragakis, E. M. (2017). Experimental Fragility Analysis of Pressurized Fire Sprinkler Piping Systems, *Journal of Earthquake Engineering*, Vol. 21 , Iss. 1.
- ICC Evaluation Service (ICC). (2010). AC 156 acceptance criteria for seismic certification by shake table testing of nonstructural components, *ICC Evaluation Service*, Whittier, CA.
- Ju, B. S., and Gupta, A. (2012). Seismic fragility of piping system. *Doctoral Dissertation*, Dept. of Civil and Environmental Engineering, North Carolina State Univ., Raleigh, NC.

- Martinez, G. E. S., and Hodgson, I. C. (2007). A comparative study of a piping system subjected to earthquake loads using finite element modeling and analysis. *Proc., 2007 Earthquake Engineering Symp. for Young Researchers*, MCEER, Buffalo, NY.
- Miranda, E., Mosqueda, G., Retamales, R., and Pekcan, G. (2012). Performance of nonstructural components during the February 27, 2010 Chile earthquake. *Earthquake Spectra*, Oakland, CA.
- Mizutani, K., Kim, H., Kikuchi, M., Nakai, T., Nishino, M., and Sunouchi, S. (2012). The damage of the building equipment under the 2011 Tohoku pacific earthquake. *9th Int. Conf. on Urban Earthquake Engineering and 4th Asia Conf. on Earthquake Engineering*, CUEE, Tokyo Institute of Technology, Tokyo, Japan.
- NFPA13. (2011). Standard for the installation of sprinkler systems, 2010 Ed., *National Fire Protection Association*, Quincy, MA.
- Nielson, G. B., and DesRoches, R. (2007). Analytical seismic fragility curves for typical bridges in the central and southeastern United States. *Earthquake Spectra*, 23(3), 615–633.
- Open system for earthquake engineering simulation (OpenSees). (2017). PEER (September 21, 2017).
- Ramanathan, K. N. (2012). Next generation seismic fragility curves for California bridges incorporating the evolution in seismic design philosophy. *Doctoral dissertation*, School of Civil and Environmental Engineering, Georgia Institute of Technology, Atlanta.
- Soroushian, S., Zaghi, A. E., Wieser, J., Maragakis, E. M., Pekcan, G., and Itani, M. (2011). Seismic analysis of fire sprinkler systems. *Eighth Int. Conf. on Structural Dynamics EURO-DYN 2011*, K.U.Leuven, Leuven, Belgium.
- Soroushian, S., et al. (2012). Seismic response of ceiling/sprinkler piping nonstructural systems in NEES TIPS/NEES nonstructural/NIED collaborative tests on a full scale 5-story building. *Proc., of 43rd Structures Congress*, ASCE, Reston, VA.
- Soroushian, S. (2013). Analytical seismic fragility of fire sprinkler piping systems. *Ph.D. dissertation*, Dept. of Civil and Environmental Engineering, Univ. of Nevada, Reno, NV.
- Soroushian, S., Zaghi, A. E., Maragakis, E. M., Echevarria, A., Tian, Y., Filiatrault, A., (2015a). Analytical Seismic Fragility Analyses of Fire Sprinkler Piping Systems with Threaded Joint, *EERI*, Vol. 31, No. 2, pp. 1125-1155.
- Soroushian, S., Zaghi, A. E., Maragakis, E. M., Echevarria, A., Tian, Y., Filiatrault, A., (2015b). Seismic Fragility Study of Fire Sprinkler Piping Systems with Grooved Fit Joints, *Journal of Structural Engineering*, ASCE, 141(6), 04014157.
- Taghavi, S., and Miranda, E. (2003). Response assessment of nonstructural building elements. *PEER Rep. 2003/05, Pacific Earthquake Engineering Research Center (PEER)*, Univ. of California, Berkeley, CA.
- Tian, Y. (2012). Experimental seismic study of pressurized fire suppression sprinkler piping system. *Doctoral dissertation*, Dept. of Civil and Environmental Engineering, State Univ. of New York at Buffalo, Buffalo, NY.
- Tian, Y., Filiatrault, A., and Mosqueda, G. (2014). Experimental seismic fragility of pressurized fire suppression sprinkler piping joints. *Earthquake Spectra*: Vol. 30, No. 4, pp. 1733-1748.
- USG Corporation (USG). (2006). Seismic ceiling resources center. (<http://www.usg.com/rc/technicalarticles/seismic-technical-guide-hanger-wire-attachment-en-SC2522.pdf>) (September. 21, 2017).
- Zaghi, A. E., Maragakis, E. M., Itani, A., and Goodwin, E. (2012). Experimental and analytical studies of hospital piping subassemblies subjected to seismic loading. *EERI*, 28(1), 367–384.